

# STOCHASTIC COOLING OF A HIGH ENERGY COLLIDER

M. Blaskiewicz\*, J. M. Brennan, R.C. Lee, K. Mernick  
BNL 911B, Upton, NY 11973, USA

## INTRODUCTION

Gold beams in RHIC revolve more than a billion times over the course of a data acquisition session or store. During operations with these heavy ions the event rates in the detectors decay as the beams diffuse. A primary cause for this beam diffusion is small angle Coloumb scattering of the particles within the bunches. This intra-beam scattering (IBS) is particularly problematic at high energy because the negative mass effect removes the possibility of even approximate thermal equilibrium [1, 2].

Stochastic cooling can combat IBS [3, 4]. A theory of bunched beam cooling was developed in the early eighties [5, 6, 7] and stochastic cooling systems for the SPS [8, 9] and the Tevatron [8, 10, 11] were explored. Cooling for heavy ions in RHIC [12, 13, 14] was also considered.

To illustrate the general principles of stochastic cooling consider  $N \gg 1$  harmonic oscillators with frequencies  $\Omega_j = \Omega_0 + \omega_j$ , with  $|\omega_j| \ll \Omega_0$ . The equation of motion for oscillator  $j$  is

$$\ddot{x}_j + \Omega_j^2 x_j = -\frac{2g\Omega_0}{N} \sum_{m=1}^N \dot{x}_m, \quad (1)$$

where  $\dot{x} = dx/dt$  and  $g$  is the cooling gain. Set  $x_j = a_j \exp(-\lambda t - i\Omega_0 t)$  and keep leading order terms to yield

$$(\lambda - i\omega_j)a_j = \frac{g\Omega_0}{N} \sum_{m=1}^N a_m. \quad (2)$$

The dispersion relation is then

$$1 = \frac{g\Omega_0}{N} \sum_{j=1}^N \frac{1}{\lambda - i\omega_j}. \quad (3)$$

Let the coarse grained, normalized distribution for the frequencies be  $f(\omega)$  and limit the discussion to the case where

$$\int_{-\infty}^{\omega_j} f(\omega) d\omega = \frac{j - 1/2}{N}, \quad (4)$$

so that the frequencies are nearly evenly spaced when viewed over short ranges of  $\omega$ . In the vicinity of frequency  $\omega$  the spacing is  $\Delta\omega = 1/(Nf(\omega))$ . Assume the existence of an inertial range  $M$  with  $1 \ll M \ll N$ . Consider

a solution to equation (3) with  $|Im(\lambda) - \omega_K| \lesssim \Delta\omega_K = 1/Nf(\omega_K)$ . For frequencies near  $\omega_K$  the sum in (3) resembles a "picket fence," while for frequencies far from  $\omega_K$  the sum is well approximated by an integral. Then

$$\begin{aligned} & \sum_{m=1}^N \frac{1}{\lambda - i\omega_m} \\ &= \sum_{|m-K| < M} \frac{1}{\lambda - i\omega_m} + \sum_{|m-K| \geq M} \frac{1}{\lambda - i\omega_m} \\ &\approx \sum_{|m| < M} \frac{1}{\lambda - i\omega_K - im\Delta\omega_K} + \sum_{|m-K| > M} \frac{i}{\omega_m - \omega_K} \\ &\approx \sum_{k=-\infty}^{\infty} \frac{1}{\lambda - i\omega_K - ik\Delta\omega_K} \\ &+ iN \int_{-\infty}^{\infty} \frac{\omega - \omega_K}{0^+ + (\omega - \omega_K)^2} f(\omega) d\omega. \end{aligned} \quad (5)$$

Use the identity

$$\lim_{M \rightarrow \infty} \sum_{k=-M}^M \frac{1}{z - ik} = \pi \frac{\exp(2\pi z) + 1}{\exp(2\pi z) - 1},$$

set

$$X(\omega_K) = \Omega_0 \int_{-\infty}^{\infty} \frac{\omega - \omega_K}{0^+ + (\omega - \omega_K)^2} f(\omega) d\omega,$$

and set  $R(\omega_K) = \pi\Omega_0 f(\omega_K)$  to obtain

$$\exp[2\pi N f(\omega_K)(\lambda - i\omega_K)] = \frac{1 + gR - igX}{1 - gR - igX}. \quad (6)$$

The right hand side of (6) is independent of  $N$  so  $Re(\lambda) \propto 1/N$ . Optimal cooling occurs for  $gR_{max} \approx 1$  with  $\min(Re(\lambda)) \approx 1/2\pi N f_{max} = \Delta\omega/2\pi N$ , where  $\Delta\omega$  is the equivalent width of the distribution. In RHIC the effective number of particles is the peak beam current per unit charge  $I_{peak}/q$  divided by the bandwidth of the cooling system  $W$ ,  $N = I_{peak}/qW$  where  $q$  is the charge per ion. The spread in intrinsic frequencies is related to the time it takes for a typical particle to slide within the bunch by  $1/W$ . This is parameterized by the mixing factor  $M$  with  $\Delta\omega = \omega_0/M$ , with  $\omega_0$  the angular revolution frequency of an on-energy particle. More accurate analytic estimates [4] as well as direct particle simulations [15] support this result.

\*blaskiewicz@bnl.gov

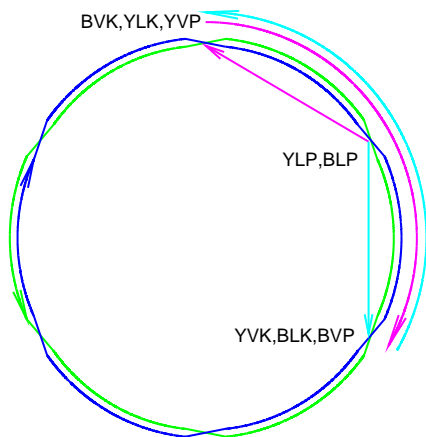


Figure 1: Locations of stochastic cooling system components. The blue vertical kicker (BVK), yellow longitudinal kicker (YLK) and yellow vertical pickup (YVP) are in the 12 o'clock straight sections. The blue and yellow longitudinal pickups (BLP, YLP) are in the 2 o'clock straight sections. The yellow vertical kicker (YVK), blue longitudinal kicker (BLK) and blue vertical pickup (BVP) are in the 4 o'clock straight sections. The yellow beam path is green and yellow signal paths are magenta. The blue beam path is dark blue and blue signal paths are light blue.

## THE RHIC COOLING SYSTEMS

A longitudinal stochastic cooling system for RHIC was commissioned in 2007 [16] and transverse cooling was achieved in 2010 [17]. The locations of the cooling components in the yellow (counterclockwise) and blue (clockwise) RHIC rings are illustrated in Figure 1 and parameters are given in Table 1. The blue vertical pickup is located in the 4 o'clock straight section. The signal is transmitted against the beam direction via an analog fiber optic link to the kicker in the 12 o'clock straight section. The bunch cores are 5 ns long and separated by 107 ns. We exploit this difference between bunch length and bunch separation by employing a Fourier series based technique. The kicker is a set of 16 cavities with resonant frequencies 4.7, 4.9, . . . 7.7 GHz. The cavities are driven by a signal,

$$S_{\perp}(t) = G_{\perp} \sum_{k=0}^{15} (-1)^k D(t - k\tau - T_{del}), \quad (7)$$

where  $D(t)$  is the difference signal out of the vertical pickup [18, 11],  $G_{\perp}$  is a gain,  $\tau = 5.000$  ns and  $T_{del}$  is adjusted so that the bunch arrives just as the cavity voltage peaks. The yellow vertical cooling system uses frequencies 4.8, 5.0, . . . 7.8 GHz and there is no factor of  $(-1)^k$  in the sum for its low level drive. Previously the blue and yellow system used the same set of cavity frequencies but this resulted in multipath problems where the signal from the yellow kicker traveled through the beam pipe to the blue pickup. This signal drove the blue kicker resulting in signals reaching the yellow pickup. Hence the signal at

the yellow pickup was partly due to the signal on the yellow beam and partly due to the signal traveling through the blue cooling system. We could not run both systems simultaneously. By using different resonant frequencies in the two rings this problem is avoided and we now run both systems at the same time. For both systems the signal is split into 16 different channels and each channel is filtered to deliver a single line. The phase and amplitude of each channel are adjusted periodically to maintain optimal cooling. Each channel then drives a narrow band 40 W solid state amplifier and subsequently a cavity. The cavities have two cells running in  $\pi$  mode. For a vertical ( $y$ ) kicker there is a longitudinal electric field

$$E_{\parallel} \sim \sin(2\pi y/w) \cos(\pi x/h), \quad (8)$$

where  $|x| < h/2$  and  $|y| < w/2$  within the cell and the closed orbit is at  $x = y = 0$ . The vertical kick follows from the Panofsky-Wenzel theorem and, depending on the cavity, is due to an electric or magnetic field. The cavities have a bandwidth of approximately 10 MHz, the inverse of the bunch spacing. The relative location of pickup and kicker are chosen so that vertical beam offsets at the pickup evolve into angular offsets at the kicker, which are then corrected by the kicker. At this time we have vertical pickups and kickers. The horizontal emittance is cooled by coupling the vertical and horizontal betatron oscillations. This is most easily seen with a simple coupled oscillator model. Let  $y$  denote the vertical dimension which has a weak damping term and  $x$  be the horizontal, undamped dimension. Introduce a weak skew coupling with potential  $\propto xy$ . Then

$$\ddot{x} + (\bar{\omega} + \delta)^2 x = 2\bar{\omega}qy \quad (9)$$

$$\ddot{y} + (\bar{\omega} - \delta)^2 y = 2\bar{\omega}qx - 4\alpha\dot{y} \quad (10)$$

where  $\bar{\omega}$  is the (large) average frequency,  $2\delta$  is the bare frequency split,  $q$  controls the coupling and  $\alpha$  determines the (very slow) cooling rate in  $y$ . The solutions are of the form  $x = \hat{x} \exp(-i\bar{\omega}t - \lambda t)$  with

$$\lambda \approx -\alpha \pm \sqrt{-q^2 + (\alpha - i\delta)^2}. \quad (11)$$

If  $|q| \gg |\alpha| + |\delta|$ , the decay rates of both modes are nearly  $-\alpha$ . For RHIC  $\alpha \sim 1/10$ min and  $q, \delta \sim$  kHz. In practice it is very easy to introduce sufficient coupling.

The blue longitudinal cooling system employs a microwave link to send the pickup signal from the 2 o'clock straight section to the 4 o'clock straight section. It employs a Fourier decomposition technique using frequencies 6.0, 6.2, . . . 8.8, 9.0 GHz. The low level drive begins as

$$S_{\parallel}(t) = \sum_{k=0}^{15} I(t - k\tau - T_{del}) - I(t - k\tau - T_{del} - T_{rev}), \quad (12)$$

where  $T_{rev}$  is the revolution period for an ideal particle and  $I(t)$  is the beam current signal. The delayed signal is required so that the voltage on the cavity will be proportional

parameter	value
$360f_{rev}$ rf voltage, frequency	300 kV, 28 MHz
$2520f_{rev}$ rf voltage, frequency	3 to 5 MV, 197 MHz
initial FWHM bunch length	2.4 ns
initial rms momentum spread	$\sigma(p)/p = 1.5 \times 10^{-3}$
particles/bunch	$10^9$
beam Lorentz factor	107
circumference	3834 m

Table 1: Machine and Beam Parameters for Gold

to the rate at which the distribution is changing, with the sign chosen to damp out the changes. The total root mean square kicker voltage is 3 kV.

The yellow systems are similar to the blue systems though differing in technical details and implementation involved several challenging problems. We took a pipe radius of 1 cm for most of the cavities, the 9 GHz longitudinal cavity had a pipe radius of 9.6 mm. This allowed for adequate beam apertures and reasonable cooling rates. To reduce aperture limitations during injection and acceleration the kicker cavities are split along the beam axis and are closed only after reaching store. The vacuum vessels and motors for the longitudinal systems were supplied by FNAL and retrofitted for our application. The vertical kickers use specifically designed vacuum vessels.

The gains and phases of the individual cavities are updated periodically during the store. This is done by first measuring the open loop system transfer function  $B(f)$ . A target transfer function  $B_0(f)$  is stored in the memory of the network analyzer. The gain and phase settings are updated to restore the reference transfer function. The system steps through all the cavities. The one turn delay filters in the longitudinal systems also undergo periodic adjustment. The network analyzer monitors the frequency of a zero of the notch filter. Thermal drifts of the delay time are compensated with a piezoelectric line stretcher. The accuracy of the delay is kept to  $\Delta t/T_{rev} \leq 2 \times 10^{-8}$ . In addition the longitudinal systems employ a fast feedback loop to compensate for antenna vibrations and phase noise in the local oscillator of the microwave link. More details of the system can be found in [19, 20, 21]. Comparison with simulations and plans for the transverse cooling system can be found in [22, 15]. While most of the simulation results are in line with earlier expectations one fortuitous difference was found. Longitudinal diffusion due to cooling and IBS results in all particles remaining at large synchrotron amplitude for a significant fraction of the time. Transverse cooling rates vanish at small synchrotron amplitude so the diffusion in synchrotron amplitude led to uniform transverse cooling. Earlier studies for the CERN SPS concluded that an extra rf system was required for uniform transverse cooling [9].

Figure 2 shows the effect of cooling on collision rates at one of the RHIC experiments. The initial luminosity is the same for both cases but cooling greatly reduces luminosity

**01 Circular Colliders**

**A01 Hadron Colliders**

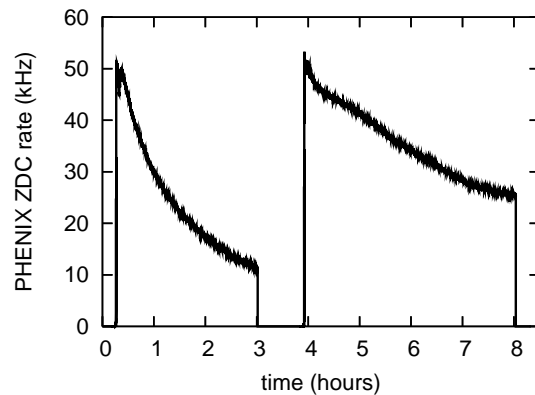


Figure 2: Zero degree calorimeter rates for adjacent stores with no cooling (left) and full cooling (right). Other parameters were as similar as possible.

decay. The net effect of cooling is to double the number of events recorded.

## SIMULATIONS AND COMPARISON WITH DATA

The cooling systems have been designed and analyzed using simulations. The simulation algorithm exploits the fact that, for fixed gain and bandwidth, the cooling time is proportional to the number of particles [3, 4, 5, 6, 7, 23]. In a simulation we are free to reduce the number of particles below the value in the actual beam by a factor  $R$ . This reduces both the number of macro-particles, and the number of turns needed to simulate one cooling time by  $R$ . The IBS is handled by using handbook formulae [1] to calculate the growth rates for the rms bunch parameters. The longitudinal profiles are decidedly non-gaussian so the diffusion rates are scaled in proportion to the local line density. Random IBS kicks are applied to the macro-particles each turn. Both transverse dimensions are tracked and a single skew quadrupole models the betatron coupling required to cool both dimensions. The stochastic cooling feedback loop is treated using a Green's function approach and implemented via a fast Fourier transform. The convergence of the simulations with the number of macro-particles has been checked. For RHIC parameters, varying the macro-particle number from 5000 to 500,000 changed the cooling rate by only a few percent [15]. It was useful to obtain Schottky spectra from the simulations. Consider the transverse cooling system. The signal at the pickup consists of a string of delta functions that occur in a burst every turn. The simulation accumulates

$$z_n = \sum_{k=1}^{N_p} x_k(n) e^{i\omega_c \tau_k(n)}, \quad (13)$$

where there are  $N_p$  macro-particles with coordinates  $x_k(n)$  and arrival times  $\tau_k(n)$  on turn  $n$ . The frequency  $\omega_c$  is the revolution line closest to the frequency of interest. The

spectrum is given by

$$S(\omega) = \left\langle \left| \sum_{n=1}^{N_{spec}} z_n e^{i(\omega - \omega_c)nT_{rev}} \right|^2 \right\rangle,$$

where  $N_{spec}$  controls the resolution bandwidth of the FFT and the angular bracket average is over several adjacent intervals.

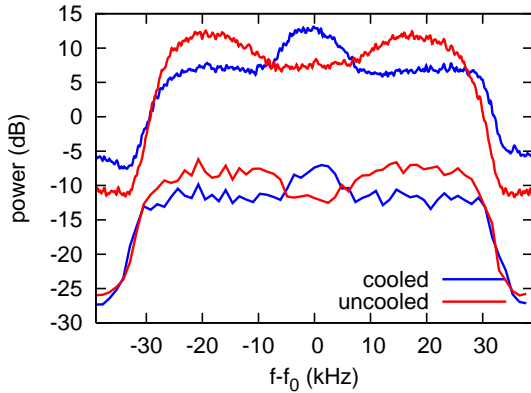


Figure 3: Measured and simulated vertical signal suppression near 5.7 GHz. The simulation is 20 dB below the data.

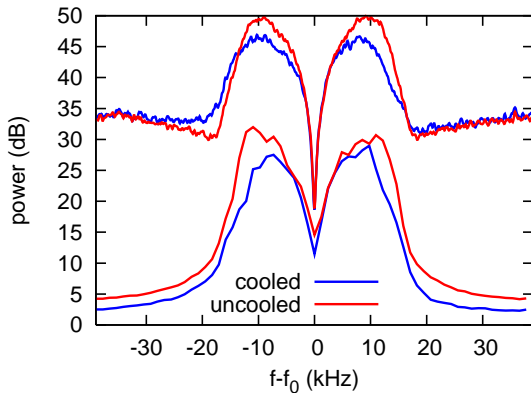


Figure 4: Measured and simulated longitudinal signal suppression near 6.4 GHz. The simulation is 20 dB below the data.

Figures 3 and 4 show measured and simulated signal suppression for the blue beam. The gain in the simulation was adjusted to be the same as the data. The ionization profile monitor data [24] for the same store are shown in Fig 5. All cooling systems were operating. Betatron coupling efficiently transfers cooling into the blue horizontal plane, yellow beam behaved similarly.

Longitudinal profiles are shown in Fig 6. The simulated profiles include losses out of the rf bucket and burn-off. The data appear to indicate a momentum aperture not included in the simulations. Because of this discrepancy the simulated luminosity is larger than the real luminosity. Figure 7 compares the integrated luminosity with an without

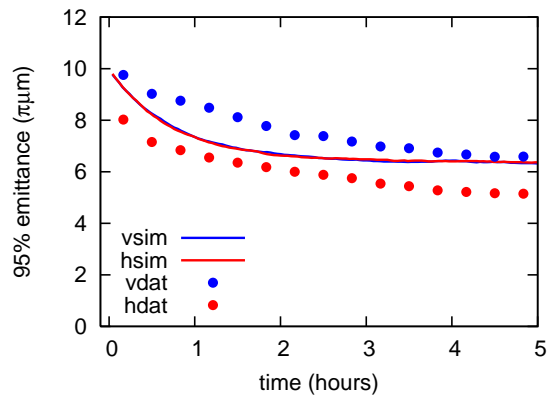


Figure 5: Evolution of normalized emittance during a store with full cooling. The blue vertical (vdat) and horizontal (hdat) are shown along with a simulation.

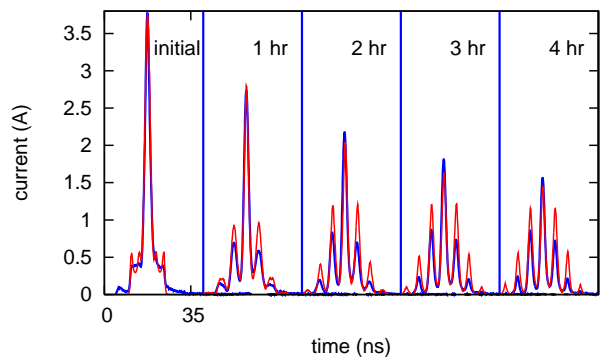


Figure 6: Evolution of the longitudinal profiles. The blue traces are data, the red traces are simulation.

cooling for stores of figure 2. The simulations were done using accurate initial conditions and then both the cooled and uncooled results were scaled by the same factor to make the simulated and real uncooled results the same. The simulations predict an 87% increase in integrated luminosity while the data show 61%. That is to say, the system delivered 70% of what was promised.

### COOLING POSSIBILITIES FOR THE LHC

Stochastic cooling of lead ions at injection is considered. Transverse cooling is fairly straightforward with a 5-8 GHz bandwidth system very similar to what is in RHIC, Fig 8. Longitudinal cooling is more difficult. We restrict discussion to 2/3 turn delay to allow the cooling signal to travel in the tunnel. This required cascaded one turn delay filters as was first done in RHIC. With an upper frequency of 9 GHz the losses are almost as bad as not cooling, Figure 9. Pushing the upper frequency to 11 or 12 GHz improves things but does not stop losses out of the bucket.

We thank Dave McGinnis and Ralph Pasquinelli of FNAL; Fritz Caspers, John Jowett, and Flemming Pedersen of CERN; Wolfram Fischer, Vladimir Litvinenko, Derek Lowenstein, and Thomas Roser of BNL; and Jie Wei of

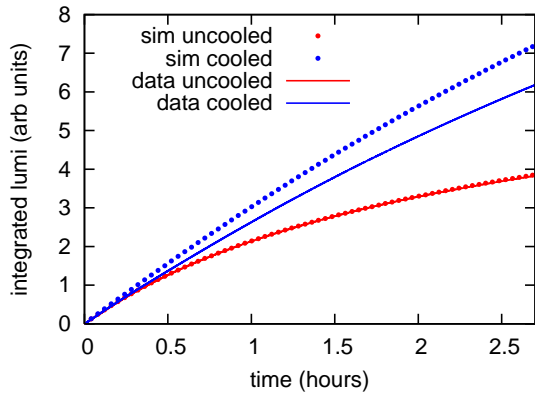


Figure 7: Comparison of integrated luminosity with and without cooling. The simulations were scaled to give good agreement for uncooled beams.

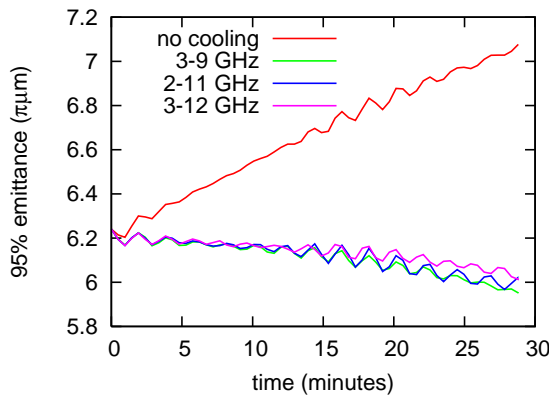


Figure 8: Transverse emittance as a function of time for uncooled beam and with transverse cooling for different longitudinal cooling frequency bands.

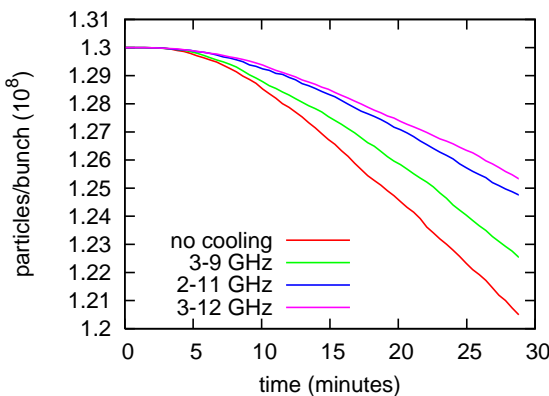


Figure 9: Bunch intensity as a function of time for uncooled beam and different longitudinal cooling frequency bands.

FRIB. The RHIC RF, Instrumentation, Controls, and Operations groups provided their characteristic high level of skill and conscientiousness. This work was performed under the auspices of the United States Department of Energy, Contract No. DE-AC02-98CH10-886.

## REFERENCES

- [1] A. Piwinski in 'Handbook of Accelerator Physics and Engineering', p 125, A. Chao, M. Tigner eds. World Scientific, 1999.
- [2] A.H. Sorensen, Lecture Notes in Physics, **400**, Springer (1992).
- [3] S. Van der Meer, *Rev. Mod. Phys* **57**, No. 3, part 1, p689 (1985).
- [4] D. Mohl, CERN 87-03, p 453 (1987).
- [5] S. Chattopadhyay, LBL-14826, (1982).
- [6] S. Chattopadhyay, *IEEE TNS* **30**, No. 4, p2646, 1983.
- [7] S. Chattopadhyay, *IEEE TNS* **30**, No. 4, p2649, 1983.
- [8] S. Chattopadhyay, *IEEE TNS* **30**, No. 4, p2334, 1983.
- [9] D. Boussard, S. Chattopadhyay, G. Dome, T. Linnecar, CERN 84-15, p197, (1984).
- [10] G. Jackson, Proceedings of the 1991 Particle Accelerator Conference, p2532, 1991.
- [11] R.J. Pasquinelli, Proceedings of the 1995 Particle Accelerator Conference, p2379 (1995).
- [12] S. Van der Meer, RHIC-AP-9 (1984).
- [13] J. Wei, A.G. Ruggiero, BNL/AD/RHIC-71 (1990).
- [14] J. Wei, Workshop on Beam Cooling, Montreux, 1993, CERN 94-03, (1994).
- [15] M. Blaskiewicz, J.M. Brennan, International Workshop on Beam Cooling and Related Topics, 2007.
- [16] M. Blaskiewicz, J.M. Brennan, F. Severino, *Phys. Rev. Lett.* **100** 174802 (2008).
- [17] M. Blaskiewicz, J.M. Brennan, K. Mernick, *Phys. Rev. Lett.* **105** 094801 (2010).
- [18] D. McGinnis, J. Budlong, G. Jackson, J. Marriner, D. Poll, Proceedings of the 1991 Particle Accelerator Conference, p1389 (1991).
- [19] J.M. Brennan, M. Blaskiewicz, PAC09, (2009).
- [20] K. Mernick, M. Blaskiewicz, J.M. Brennan, B. Johnson, F. Severino Beam Instrumentation Workshop 2010, Santa Fe, (2010).
- [21] M. Blaskiewicz, J.M. Brennan *Phys. Rev. ST Accel. Beams* **10** 061001, (2007).
- [22] M. Blaskiewicz, J.M. Brennan, F. Severino, Proceedings of the 2007 Particle Accelerator Conference, p2014 (2007).
- [23] F. Sacherer CERN-ISR-TH/78-11 (1978).
- [24] R. Connolloy, J. Fite, S. Jao, S. Tepikian, C. Trabocchi, Beam Instrumentation Workshop 2010, Santa Fe, (2010).